

Developing a New Optic Nerve Injury Model in *L. stagnalis*; Insights into Molluscan Phototactic and Visual Processing Activities *In Vivo*



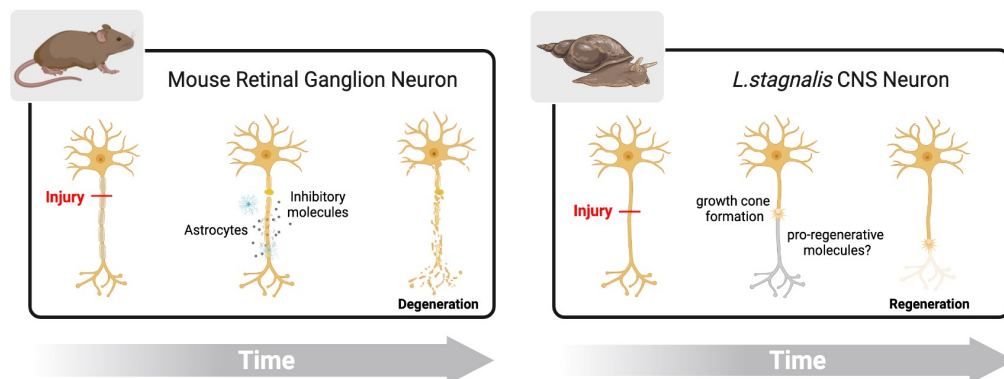
Alicia N. Harracksingh MSc.¹, Julia Bandura BSc.¹, Joseph Steinman MSc., Ph.D.¹, Meng Yang BSc.¹, Hong-Shuo Sun M.D., Ph.D.², Philippe P. Monnier MSc., MBA., Ph.D.³, Zhong-Ping Feng M.D., Ph.D.¹

1. Department of Physiology, Faculty of Medicine, University of Toronto, Toronto, Ontario, Canada.

2. Department of Physiology, Faculty of Medicine, University of Toronto, Toronto, Ontario, Canada; Department of Surgery, Faculty of Medicine, University of Toronto, Toronto, Ontario, Canada.

3. Department of Physiology, Faculty of Medicine, University of Toronto, Toronto, Ontario, Canada; Krembil Research Institute, Vision Division, Krembil Discovery Tower, Toronto, Ontario, Canada; Department of Ophthalmology and Vision Sciences, Faculty of Medicine, University of Toronto, Toronto, Ontario, Canada.

I. Unlike mammalian RGCs, *L. stagnalis* CNS neurons undergo spontaneous regeneration after injury by stimulating microtubule assembly¹



II. *L. stagnalis* as a model system for visual processing and optic nerve injury

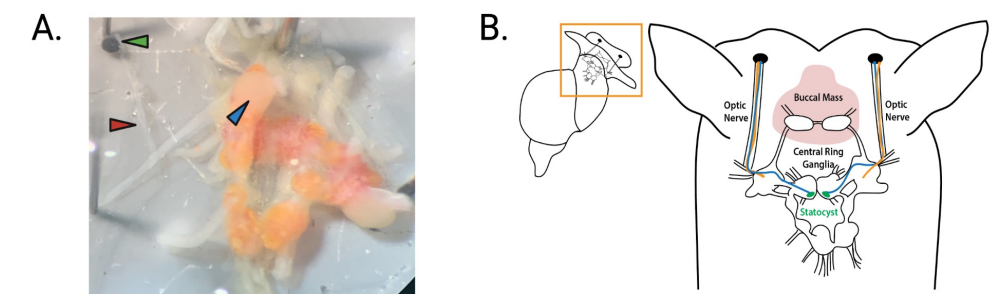


Figure 1. Schematic depiction of the *L. stagnalis* CNS and visual system. (A) Dissection of *L. stagnalis* CNS (central ring ganglia), with left cerebral ganglia depicted (blue arrow). Left optic nerve (red arrow) and eye (green arrow) are indicated. (B) General depiction of the *L. stagnalis* visual system located in the snail mantle, with optic nerves, central ring ganglia, statocyst (gravitometric sensing organ)² and buccal mass noted. Neurons known to be responsible for phototransduction and the phototactic response extending from the eye to the central ring ganglia and statocyst are indicated in orange and blue, respectively.

III. The *L. stagnalis* eye is comprised of structurally homologous anatomical features to mammals

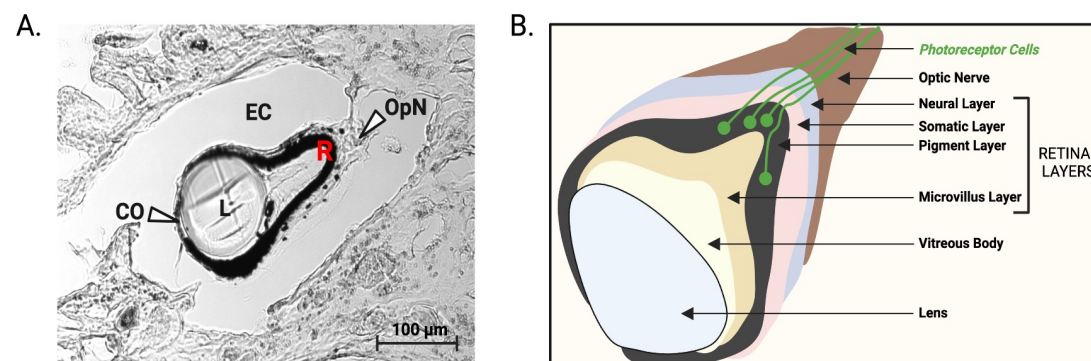
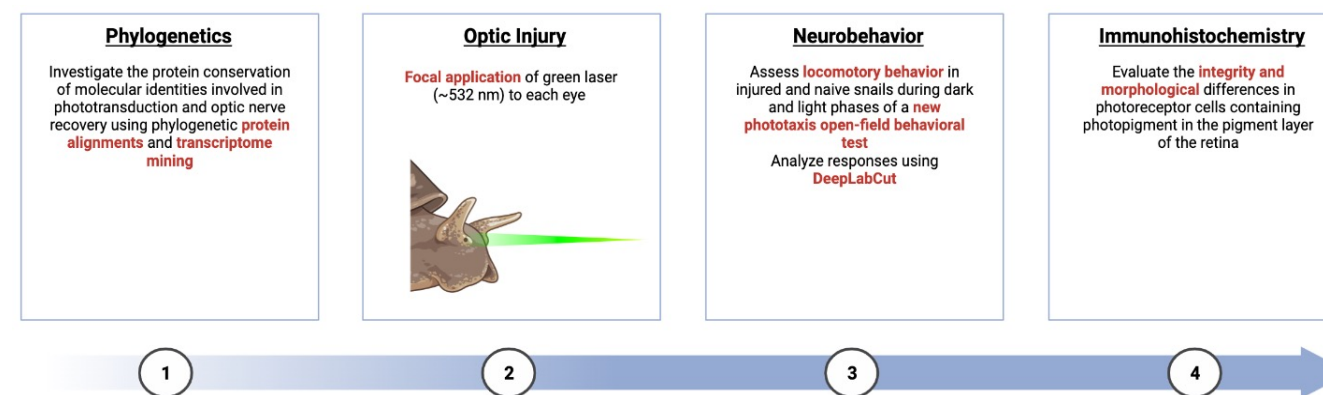


Figure 2. (A) Brightfield micrograph of the *L. stagnalis* left eye structures using brightfield microscopy (10X) reveals structurally homologous structural features to mammals. CO, cornea; EC, eye capsule; L, Lens; OpN, optic nerve; R, retina. *L. stagnalis* mantle tissue was dissected under lit conditions, fixed in 4% paraformaldehyde, embedded in OCT and sectioned (30µm) with the cryostat. Slice through the tissue is as relative to embedded tissue positioning. Images were acquired using Zeiss LM-500 confocal microscope, and scale bar is indicated. (B) Schematic depiction of the *L. stagnalis* eye depicts anatomical features of the eye. The lens, vitreous body, retinal layers (microvillus, pigment, somatic, and neural), and optic nerve are indicated. Photoreceptor cells extending from the pigment layer through the optic nerve to the central ring ganglia are indicated (green)³.

IV. Rationale and Objective

While it is thought that phototactic behaviors are due to photoreceptor activation in the retina, the downstream signaling cascades have not been well-identified. As well, *L. stagnalis*' response to *in vivo* optic injury phototactically has not been investigated, due largely to a lack of suitable experimental models. Establishing a robust pipeline to assess molluscan phototactic and visual processing activities allows us to develop and verify systematic protocols to study neurobehavioral and phototactic activities of *L. stagnalis*

V. Methods for assessing neurobehavioural and phototactic activities in *L. stagnalis*



VI. Presence of retinal rhodopsin in *L. stagnalis* supports the conservation of phototransduction pathways in mollusks

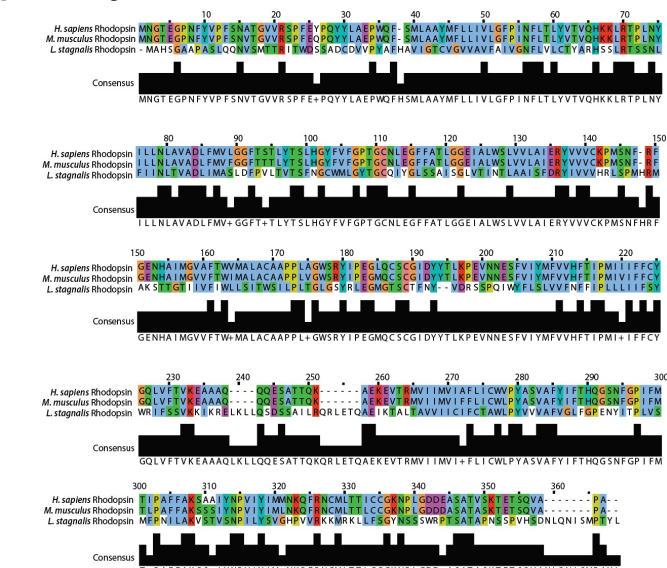


Figure 3. Rhodopsin is conserved in *L. stagnalis*. Conservation of Rhodopsin reveals conservation between homologs from *H. sapiens*, *M. musculus*, and *L. stagnalis*. Muscle alignments⁴ were completed between *H. sapiens*, *M. musculus* and the predicted homologs from *L. stagnalis* using our group's refined transcriptome⁵ and analyzed using Jalview Software⁶. *H. sapiens* and *M. musculus* sequences were obtained from the NCBI database; *H. sapiens* Rhodopsin (NP_000530.1) and *M. musculus* Rhodopsin (NP_663358.1).

VII. Rhodopsin is present in *L. stagnalis* central ring ganglia and mantle/eyes

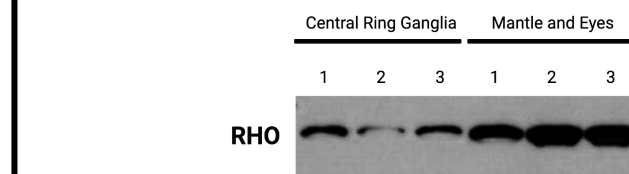
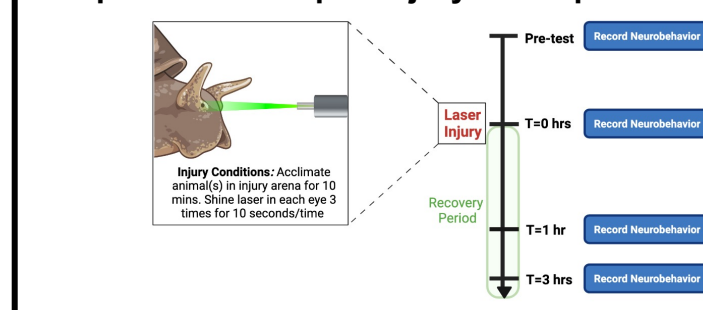


Figure 3. Rhodopsin is present in the central ring ganglia and mantle with eyes of *L. stagnalis*. Western blot of total ganglionic and mantle with eyes protein lysate showing that the rabbit anti- Octopus rhodopsin (1:1000; CosmoBio) recognizes a single protein with a molecular weight of 40 kDa corresponding to the predicted molecular weight of rhodopsin (RHO) in *L. stagnalis*

VIII. Focal application of green laser to target the function of rhodopsins in *L. stagnalis* and produces an optic injury to the photoreceptors



IX. Developing a phototaxis response neurobehavioral pipeline to assess ocular photoactive response in *L. stagnalis* after optic laser injury using DeepLabCut

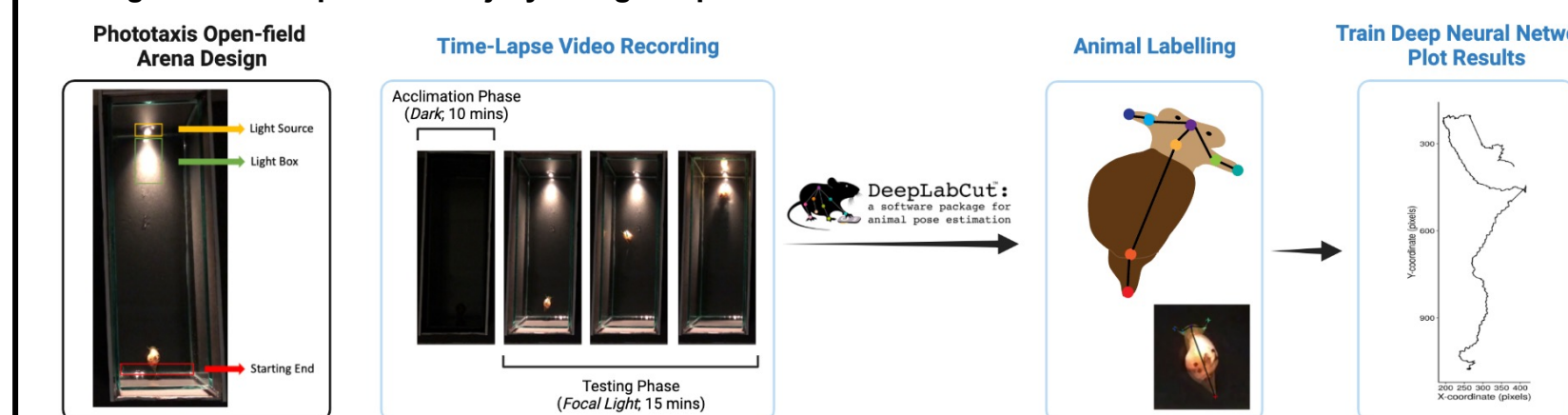


Figure 5. DeepLabCut software can be used to create a deep neural network that can estimate *L. stagnalis* locomotory activity in videos acquired from the phototactic response neurobehavioral assays. A phototaxis open-field arena containing a light source and designated light box was created to test the movement of an animal from the start end toward the light source. During the phototaxis neurobehavioral testing, time-lapse video recordings were taken during an acclimation phase in the dark (10 mins), after which a snail is returned to the starting end, and a testing phase in the light (15 mins) commences. After acquisition of the recording, videos are processed in a DeepLabCut^{7,8} machine learning model, where snails are labelled at various anatomical points on their body and the XY-coordinates of the labelled points can be plotted. Using labelled videos, a deep neural network can be trained to 'learn' animal locomotory movement in the open-field arena.

X. PRELIMINARY: Assessing the phototaxis response and potential for photoreceptor recovery in *L. stagnalis* before and after optic laser injury

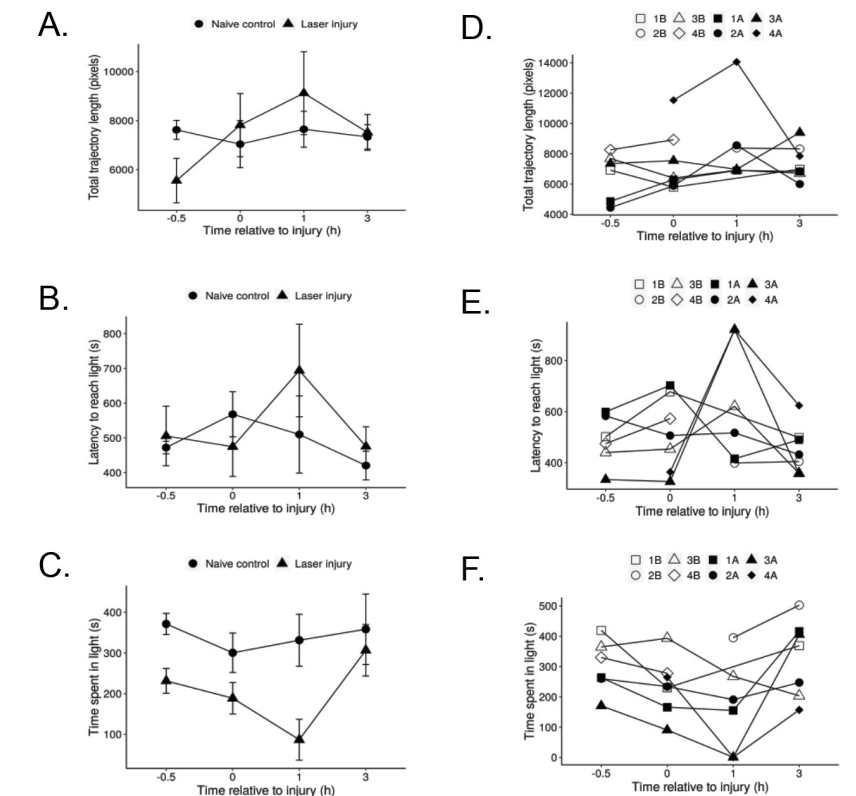


Figure 6. Locomotory patterns of *L. stagnalis* during phototaxis response testing in naive control and laser injury snails. Single-blind analyses of phototaxis neurobehavioral testing of snails, aged 5-months, in naive control (n=4) and laser injured (n=4) groups. Analysis of plots depict mean outcomes and SEM of (A) total trajectory lengths of travel during the testing period, in pixels, (B) latencies to reach a fixed, designated light box within the phototaxis arena, in seconds, and (C) time spent in the designated light box during the testing period, in seconds, in naive control and laser injured snails. Individual outcomes for naive control (1B-4B) and laser injured (1A-4A) snails depicts (D) total trajectory lengths of travel during the testing period (pixels) (E) latencies to the designated light box (secs) and (F) time spent in the designated light box (secs). Time-lapse video data was labelled and analyzed using the DeepLabCut machine learning pipeline and line graphs were generated in R coding software⁹.

XI. Conclusions and Future Directions

- This study will establish a new *in vivo* model to study neurobehavioral and phototactic activities of *L. stagnalis*. Furthermore, this model will allow us to probe for new signalling molecules and cascades involved in the *L. stagnalis* pro-regenerative response in the optic nerve that could be evolutionarily conserved in mammals
- Future experiments will use immunohistochemistry to investigate the integrity of the retina in naive control and laser injury animals
- Future studies will determine how the pro-regenerative molecules that promote microtubule assembly in *L. stagnalis* CNS neurons function in optic nerve injury through *in vitro* and *in vivo* assays

XII. Significance

We anticipate that this work will enable us to deduce new molecular and cellular cascades involved in optic nerve regeneration. Probing these cellular and molecular cascades underlying optic injury and regeneration in *L. stagnalis* will allow us to further probe new cellular and molecular identities involved in visual system processing and regeneration in mammals.

XIII. References

1. Nejabatkah, N., Guo, C. H., Lu, T. Z., Pei, L., Smit, A. B., Sun, H. S., ... & Feng, Z. P. (2011). Caltinin, a novel molluscan tubulin-interacting protein, promotes axonal growth and attenuates axonal degeneration of rodent neurons. *Journal of Neuroscience*, 31(43), 15231-15244.
2. Sakakibara, M., Arakaki, T., Iizuka, A., Suzuki, H., Horikoshi, T., & Lukowiak, K. (2005). Electrophysiological responses to light of neurons in the eye and statocyst of *Lymnaea stagnalis*. *Journal of Neurophysiology*, 93(1), 493-507.
3. Zieger, M. V., & Meyer-Rochow, V. B. (2008). Understanding the cephalic eye of pulmonate gastropods: a review. *American Malacological Bulletin*, 26(1/2), 47-66.
4. Edgar, R. G. (2004). *Mollusca: multiple sequence alignment with high accuracy and high throughput*. *Nucleic acid research*, 32(5), 1792-1797.
5. Ding, N., Bandura, J., Zhang, Z., Wang, Y., Labadie, K., Noel, B., ... & Feng, Z. P. (2021). Ion channel profiling of the *Lymnaea stagnalis* ganglia via transcriptome analysis. *BMC genomics*, 22(1), 1-25.
6. Waterhouse, A. M., Procter, J. B., Martin, D. M., Clamp, M., & Barton, G. J. (2009). *Jalview Version 2—a multiple sequence alignment editor and analysis workbench*. *Bioinformatics*, 25(9), 1189-1191.
7. Mathis, A., Mamidanna, P., Cury, K. M., Abe, T., Murthy, V. N., Mathis, M. W., & Bethge, M. (2018). DeepLabCut: markerless pose estimation of user-defined body parts with deep learning. *Nature neuroscience*, 21(9), 1281-1289.
8. Nath, T., Mathis, A., Chen, A. C., Patel, A., Bethge, M., & Mathis, M. W. (2019). Using DeepLabCut for 3D markerless pose estimation across species and behaviors. *Nature protocols*, 14(7), 2152-2176.